

Treatment of coffee pulp wastewater by photocatalytic bismuth ferrite nanomaterial

Nidhi A Harish Kumar, Shivakumar Bellagere Puttaraju and N. Kumar Swami

Post graduate student, JSS Science and Technology University, Mysore

Assistant Professor, JSS Science and Technology University, Mysore

Associate Professor, JSS Science and Technology University, Mysore

Abstract - Coffee is the second most traded commodity in the world, after gasoline. With 4.5 million hectares specifically set aside for coffee production, India is the seventh largest coffee producer in the world. Both dry and wet processing methods are available for making coffee. The wet processing system produces a large volume of toxic effluents since it uses so much water, all of which may be simply dumped into a nearby river or stream. The effects of different operational parameters, such as catalyst dosage, contact time, and the addition of an oxidant, on the decrease of BOD, COD, and color were evaluated through experimentation. During an 8-hour contact period with visible lighting of 9W, a catalyst dosage of 20 mg of bismuth ferrite (BiFeO_3) was seen to remove 98% of BOD, 88% of COD, and 93% of color. The best outcomes were obtained via visible light photo catalytic degradation (9W). The findings demonstrate that the photo catalytic degradation using BiFeO_3 follows pseudo-first-order kinetics and that the majority of the degradation takes place on the surface of nanoparticles which fits in the Langmuir-Hinshelwood kinetic model.

Key Words: Coffee effluents; Photocatalytic Degradation; Bismuth Ferrite; Biological Oxygen demand; Chemical Oxygen Demand; Color.

1. INTRODUCTION

The plant genus *Coffea* is a member of the Rubiaceae family. The coffee plant's seeds, or coffee beans as they are more widely known, can be used to prepare beverages. The three types of coffee that are most often consumed worldwide are Arabica, Robusta, and Liberica (*Coffea Liberica*). Robusta has the highest caffeine level (28%) and Liberica has the lowest (2%), with Arabica having the highest quality in terms of flavor and fragrance (70%). In India, processing coffee is a seasonal endeavour that lasts for three to four months from November to February. (Coffee Board 2020).

Coffee processing wastewater is one of the agro-processing wastes that need special care because of the potential for pollution caused by the world's huge coffee production (Tekle et al., 2015). Dry and wet processing methods are available for coffee processing. The wet processing technique generates a lot of dirty effluents that may readily be dumped into a nearby stream or river because it uses a lot of water. Pulp, mucilage, and parchment are byproducts of

coffee processing in the following percentages: 43%, 13%, and 6%, respectively. Due to the high acidity and high concentrations of both suspended particles and organic components in this wastewater, treatment is particularly challenging. Due to colored effluent pollution, this pollution results in opacity, a high biological and chemical oxygen demand, eutrophication, light blocking, and disruption of photosynthesis (Coffee Board of India, 2021). The wastewater produced by the coffee producing process can be treated in a variety of methods. Adsorption, ionising radiation, electrochemical oxidation using steel electrodes, and, more recently, chemical flocculation in combination with enhanced oxidation technologies are a few of the techniques that can be used (Alemayehu et al., 2021).

The treatment of wastewater, photocatalysis has the potential to be employed for the production of power and hydrogen, as well as the reduction of atmospheric CO_2 levels (Ahmad et al., 2021). Over the years, a significant increase in the number of persons interested in finding solutions to water contamination has occurred (Siddique et al., 2018). Photocatalysis requires catalyzing photochemical reactions to start the catalytic process. A type of catalytic reaction called photocatalysis necessitates the presence of light, either visible or ultraviolet. Two extensively discussed forms of photocatalytic reactions are photocatalytic oxidation (PCO) and photocatalytic decomposition (PCD). The photodegradation of pollutants is increasingly using photocatalysts activated by visible light because sunlight makes up 40% of the visible spectrum (Weon et al., 2019).

BiFeO_3 (BFO) is an increasingly significant topic of study in contemporary scientific research due to its photocatalytic and multiferroic properties, magnetic ordering, and doping effects. A form of semiconductor with several uses is called BFO nanoparticles. Biferrous iron oxide is an example of a multiferroic material with ferroelectric and magnetic characteristics (BiFeO_3). It is hence frequently utilised in ferroelectric and magnetic devices. Chemistry, a very small band gap of 2 to 2.5 eV, a specific surface area (SSA) of 5 to 50 m^2/g , and coexisting ferroelectric and magnetic properties are all characteristics of this substance. As a result, various methods for obtaining BFO particles with desired morphologies have been studied extensively, including co-precipitation, low-temperature synthesis, the sol-method, hydrothermal method, microwave

hydrothermal method, solid-state reaction, rapid liquid-phase sintering technique, pulsed laser deposition, electrospinning, magnetron sputtering, Pecchini method, mechanochemical synthesis, and combustion.

Due to the production of contaminants and secondary phases such as $\text{Bi}_2\text{Fe}_4\text{O}_9$ and $\text{Bi}_{25}\text{FeO}_{40}$, obtaining pure BFO is difficult. The effect of calcination conditions on the structure, morphological, and magnetic properties of *BFO nanoparticles synthesized by co-precipitation technique*, with an emphasis on calcination temperature (CT) and calcination duration (CD). Co-precipitation is preferable because it produces homogenous nanosized particles at a reasonable price in a short period. As a result, secondary phases of bismuth ferrite are formed alongside the primary phase. Synthesis using the co-precipitation method can help with this issue and prevent secondary phase formation during the process. They were able to manage numerous processing parameters for the synthesis of BFO, but they were unable to eliminate impure phases (Maleki et al., 2017).

2. METHODOLOGY

2.1 Chemicals

Bismuth (III) nitrate pentahydrate ($\text{Bi}(\text{NO}_3)_3 \cdot 5\text{H}_2\text{O}$), Iron (III) nitrate nonahydrate ($\text{Fe}(\text{NO}_3)_3 \cdot 9\text{H}_2\text{O}$), Ammonia (2.5 M) (NH_3). Through the experimental studies, double-distilled deionized water was used.

2.2 Synthesis of BiFeO_3 by co-precipitation method

The process of co-precipitation was used to produce the BiFeO_3 . Typical synthesis procedures are as follows. A completely transparent solution was created by dissolving 0.004 mol of $\text{Bi}(\text{NO}_3)_3 \cdot 5\text{H}_2\text{O}$ and 0.004 mol of $\text{Fe}(\text{NO}_3)_3 \cdot 9\text{H}_2\text{O}$ in 200 mL of double-distilled water after agitating the liquid for about 20 minutes (Caglar et al., 2021). To determine the reaction outcome using a precise chemical precipitation process, several pH levels were tested using a synchronised drop of a solution containing ammonia at a concentration of 2.5 M and water at a concentration of 10 M. The precipitates were stored at room temperature for about 24 hours and then washed and filtered with double distillation water. This made it easier to remove any chemically- unreacted materials. The finished products were heated to 100°C in a hot air oven for over five hours. These powders underwent a two-hour annealing process in a kiln at 600°C . An X-ray diffractometer was employed to carry out in-depth investigation on the materials phase identification. FT-IR spectroscopy, or the Fourier transform of the infrared spectrum, was used to determine the local structure of the particles. The morphology of the generated particles was examined using energy dispersive X-ray spectroscopy (EDX) and scanning electron microscopy (SEM). BiFeO_3 particle local lattice distortions were examined using vibrational spectroscopy and Raman scattering. (Muneeswaran et al., 2013).

2.3 Photocatalytic degradation of Arabica and Robusta coffee effluent

In batch mode, for up to 48 hours at a time, the photocatalytic degradation of coffee processing effluent was investigated. This time was chosen as precautionary, considering that several pollutant compounds contained into coffee wastewater are complex molecules (for example, proteins, phenols, pectins). The photocatalytic degradation of coffee effluents was performed under visible light (LED blub with 9W). At the end of experimentation, samples of the reaction mixture were withdrawn and filtered using Whatman paper filter (grade no. 42, pore size = $2.5 \mu\text{m}$) and analyzed for BOD, COD and colour to compare it with the initially measured values of these parameters to evaluate the photocatalytic removal efficiency. Decolourization was measured as a decrease in absorbance at 250 nm by a UV-VIS double spectrophotometer. The percentage reduction in BOD, COD and colour of the samples were calculated using the following Equations, respectively: $\text{COD removal \%} = \frac{C_i - C_f}{C_i} \times 100$ where, C_i = Intial COD Concentration in effluent (mg/l), C_f = Final COD Concentration in effluent (mg/l), $\text{Colour removal \%} = \frac{C_{li} - C_{lf}}{C_{li}} \times 100$ where, C_{li} = initial colour (colour unit), C_{lf} = final colour (colour unit) and $\text{BOD removal \%} = \frac{B_i - B_f}{B_i} \times 100$ where, B_i = Intial BOD (mg/l), B_f = Final BOD (mg/l).

2.4 Kinetics model for coffee effluents

When investigating chemical or biological reactions, kinetics is concerned with reaction rates, the effects of outside factors, the rearrangement of molecules, the generation of intermediates, and the function of a catalyst in the reaction process. Kinetics also includes the study of the effects of environmental conditions. Because it provides proof for the mechanics underlying chemical reactions, kinetics is significant. Aside from the importance that reaction processes have for the scientific community, knowledge of them can help one choose the best approach for getting a response. The degradation of a coffee effluent and the reduction of a photocatalytic reactor's (BiFeO_3) catalyst were both studied using a linear kinetics order reaction kinetic (Ho Choo et al., 2018). The data obtained for the pseudo-first-order reaction kinetics of photocatalytic reduction best fit the first of the three kinetic models that were investigated. The conclusions we came at as a result of our inquiry influenced this. The following equation, which describes the Langmuir-Hinshelwood kinetic model, can be used to explain the rate of the photocatalytic reaction: The photodegradation rate constant, k , is represented by the equation $\ln \frac{A_0}{A} = t * k$.

3. RESULTS AND DISCUSSION

3.1 Characterization of BiFeO₃

3.1.1 X-Ray diffraction studies

The produced BiFeO₃ nanoparticles underwent PXRD analysis to determine their crystal structure and phase purity. The PXRD pattern for BiFeO₃ nanoparticles produced by the Co-precipitation technique is shown in Figure 1. Using the Debye-Scherrer formula $D = \frac{0.9\lambda}{\beta \cos \theta}$ where D is the average crystalline size, λ the wavelength of incident X-ray (1.5406 Å), θ the diffraction angle in degree and β the full width at maximum in radians. The calculated crystallite sizes were found to be 25 nm. BFO powders synthesised at pH 11 had lower percentage of the secondary phase.

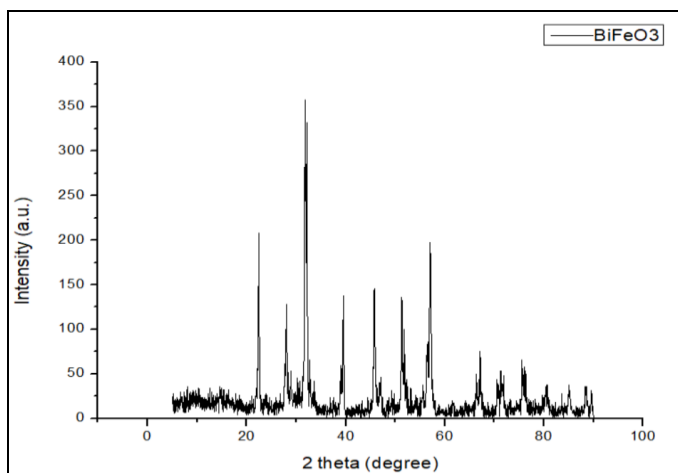


Fig 1: XRD pattern of BFO powders

3.1.2 FT-IR spectral studies

The formation of BiFeO₃ nanoparticles might be confirmed if it is possible to identify the vibrational frequencies of chemical bonding in perovskite BiFeO₃. For instance, in the 700-450 cm⁻¹ range, vibration bands linked to metal and oxygen can be found. The FTIR spectra of BiFeO₃ nanoparticles are shown in Figure 2. Octahedral FeO₆ groups with distinctive Fe-O stretching and bending vibration modes at 550 and 420 cm⁻¹, respectively, were shown to exist in crystal lattices. The characteristic IR peaks of BiFeO₃ form at higher frequencies for larger particle sizes, according to the pertinent research. In addition, the stretching and bending of water molecules on the surface, as well as their absorption by OH, are linked to the IR bands at 3000 and 1680 cm⁻¹, respectively. On the other hand, the band at 1070 cm⁻¹ can be a result of the stretching vibrations of the nitrate ions produced by HNO₃ during production.

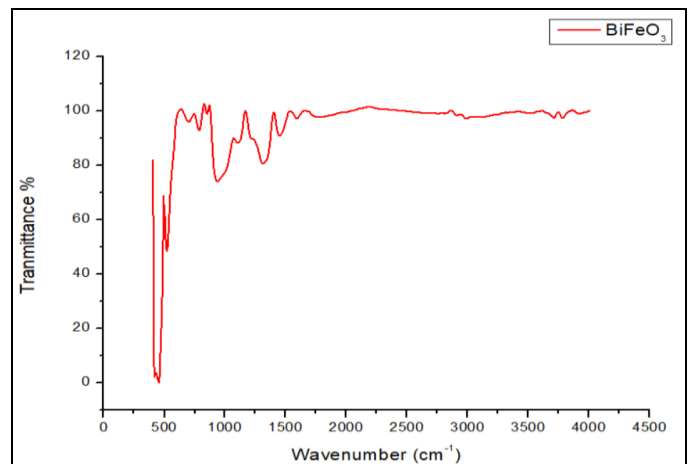


Fig 2: FTIR spectrum of BiFeO₃ nanoparticles

3.1.3 Raman analysis

Figure 3 shows room temperature of the Raman spectra of ceramics made of BiFeO₃ and microcrystals that coprecipitated (100–800 cm⁻¹). The Raman graphs were fitted with Gaussians using the Origin programming environment. The FeO₆ octahedral stretching vibration is connected to a high-frequency vibrational mode (> 400 cm⁻¹) while the Bi atoms in the perovskite unit prefer a low-frequency vibrational state, according to Raman spectra. Both of these modes have to do with vibrations. Four unique vibratory modes were discovered through research on the covalent bonds between Bi-O complexes and the distortions brought on by the Bi atoms in the tetrahedral configuration. It was found that Bi atoms produce these modes. At 269-271 cm⁻¹, the E vibrational mode displays ferroelectric distortion. At 337 cm⁻¹, 524 cm⁻¹, and 615 cm⁻¹, the internal stretching of the FeO₆ octahedron is responsible for the additional E vibrational modes. Due to lattice distortions caused by the Fe atoms in the FeO₆ octahedron, the Raman active vibrational modes (E) are pushed into a higher frequency band. The graph demonstrates that the BFO sample has a peak at 527 cm⁻¹, which emerges during analysis of the sample.

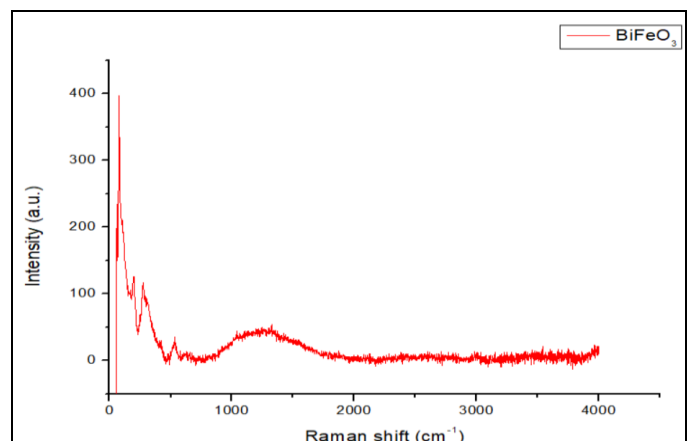


Fig 3: Raman Spectra of BiFeO₃ nanoparticles

3.1.4 Morphological characterization using SEM and EDX analyses

BiFeO₃ nanoparticles surface shape and particle size are analysed in Figure 4 using SEM images. The BiFeO₃ nanoparticles' size spans from 20 to 60 nm, which is in line with their uneven form and dispersion of grain size. This size range is suitable by Scherrer's Equation. The EDX spectrum of BiFeO₃ nanoparticles is shown in Figure 5. The chemical makeup of nanoparticles was examined using this spectrum. It was found that each of these elements has an atomic proportion of 62.10 in its natural environment. In the absence of any additional Bi-Fe phase types, BiFeO₃ nanoparticles were effectively synthesised based on the existence of only these three elements and a ratio of 1:1.15:3.24 M between bi, iron, and oxygen.

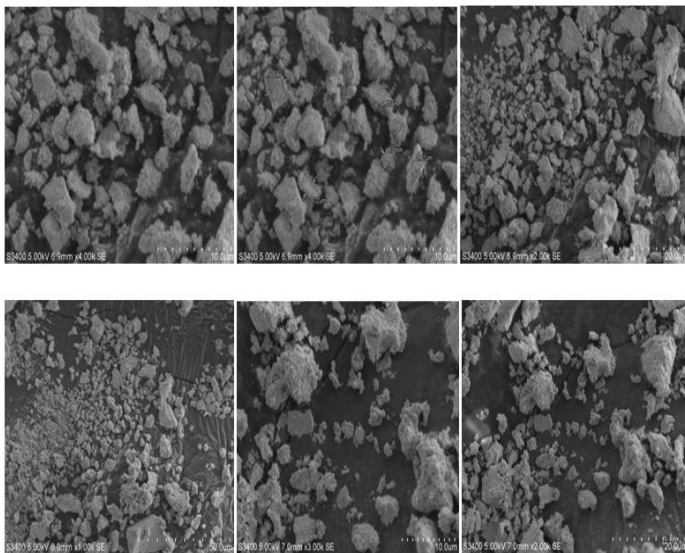


Fig 4: SEM image of BFO powders

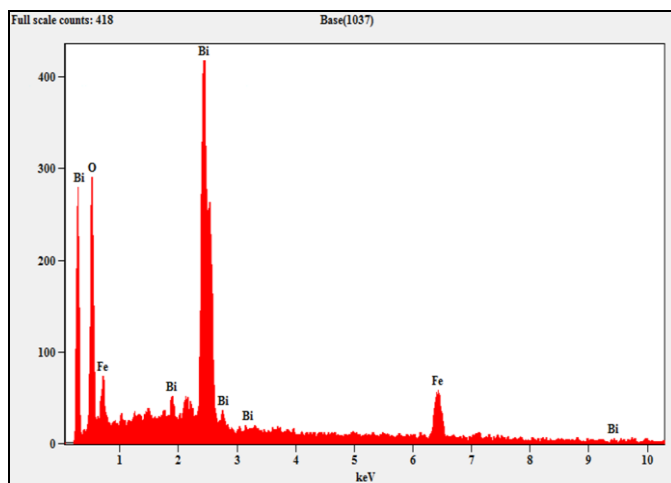


Fig 5: EDX curve of BiFeO₃ nanoparticles

3.2 Physico – chemical analysis of coffee effluents

The characteristics results of raw coffee pulping wastewater collected from 2 different sources. It can be noted that the wastewater is acidic with a high concentration of BOD, COD and colour, which imposes a challenge for the selection of treatment technology. The wastewater is characterized by high concentration of COD, nitrogen, phosphorus, BOD, color, TDS, TSS, turbidity, sulphate with low pH. The results are interpreted in the table 1.

Table -1: Characteristic of raw coffee pulping wastewater

Parameters	Coffee effluents		Prescribed limits from BIS
	Arabica	Robusta	
pH	4.58	3.59	6 – 9
TDS	148 mg/l	1752 mg/l	100 – 600 mg/l
TSS	1012 mg/l	7368 mg/l	500 – 1200 mg/l
Turbidity	310 NTU	540 NTU	<5 NTU
BOD	3082 mg/l	4082 mg/l	100 - 1000 mg/l
COD	7200 mg/l	19200 mg/l	250 mg/l
Nitrate	33.4 mg/l	435 mg/l	10 – 20 mg/l
Phosphate	68.75 mg/l	714.3 mg/l	-
Sulphate	5.02 mg/l	7.20 mg/l	2 – 5 mg/l

3.3 Treatment for coffee effluents

Over a constant test period of 20 minutes to 2880 minutes, a batch photocatalytic degradation of coffee processing effluent was carried out using a variety of different catalyst doses. The reactor is much simpler to run because to the magnetic stirrer located at the base. The reaction mixture samples were filtered using a Whatman paper filter (grade 42, 2.5 micrometres) at the conclusion of the experiment to eliminate them.

3.3.1 Effect of catalyst dosage

The experiment was conducted in a closed reactor with LED light (9W) serving as the process source for photocatalysis. Each analysis uses 100 ml of coffee effluents. Larger-surface-area nanoparticles (BFO) tended to exhibit more photocatalytic activity. Doses of BiFeO₃ range from 10 mg to 50 mg. The optimum dosage for the photocatalytic process was 20 mg, in which BOD concentration reduced from 3082 mg/l to 49.2 mg/l and percentage removal was up to 98%. COD concentration reduced from 7200 mg/l to 800 mg/l and

percentage removal was up to 88.88% and color reduced up to 96.67% and also nitrate reduced to 19.8 mg/l which is in permissible limit (for Arabica effluent). Similarly, BOD concentration reduced from 4082 mg/l to 123 mg/l and percentage removal was up to 96.92%, COD concentration reduced from 19200 mg/l to 1600 mg/l and percentage removal was up to 91.66% and color reduced up to 63.85% and also nitrate reduced from 435 to 87.9 mg/l (for Robusta effluent). The increased pollutant removal rate that follows the increase in the catalyst loading can be attributed to the fact that a more significant number of photons are adsorbed, thus accelerating the process. The results are presented in figure 6-9.

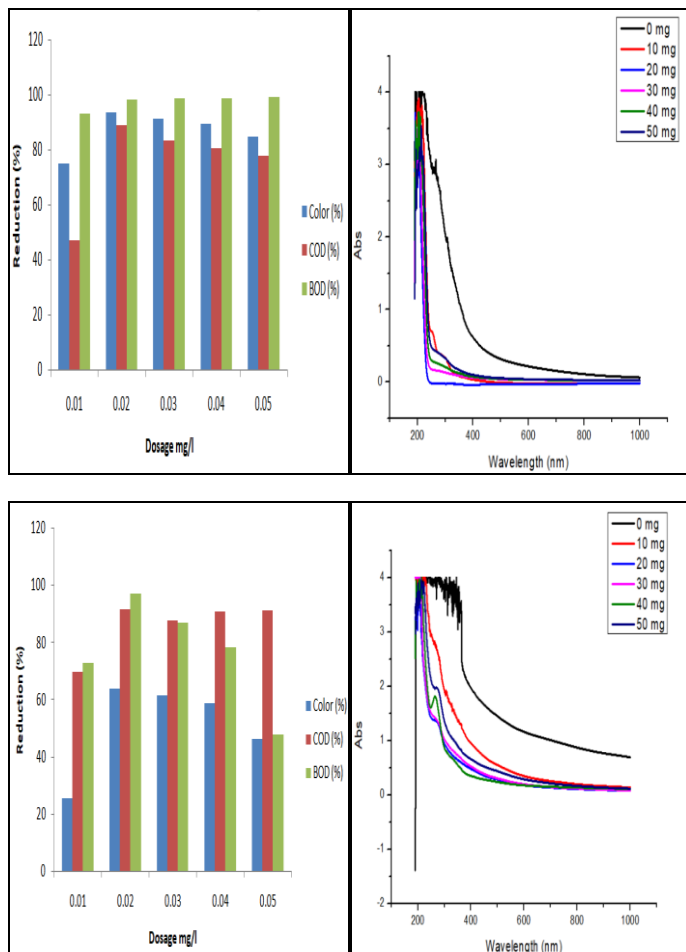


Fig 6 and 9: Reduction percentage of BOD, COD and color for different dosage of BiFeO₃, Fig 7 and 9: Degradation for different dosage of BiFeO₃ (250 nm)

3.3.2 Effect of contact time

The 20 mg, are tested with various time intervals for both Arabica and Robusta effluent. BiFeO₃ was used as the catalyst in a beaker at concentrations of 20 mg for periods ranging from 20 to 480 minutes. The optimum contact time is 8hr (480 min). The COD concentration reduced from 7200 mg/l to 800 mg/l, BOD concentration reduced from 3082

mg/l to 49.2 mg/l. The percentage removal of COD was 88.88%, BOD was 98.40% and color reduction was 96.67% for Arabica effluent treatment. Similarly the COD concentration reduced from 19200 mg/l to 1600 mg/l, BOD concentration reduced from 4082 mg/l to 123 mg/l. The percentage removal of COD was 91.66%, BOD was 96.98% and color reduction was 63.855% for Robusta effluent. Adsorption of the molecules can be seen up until 8 hours, but desorption, or the removal of the molecules, occurs after that. The results are presented in figure 10-13.

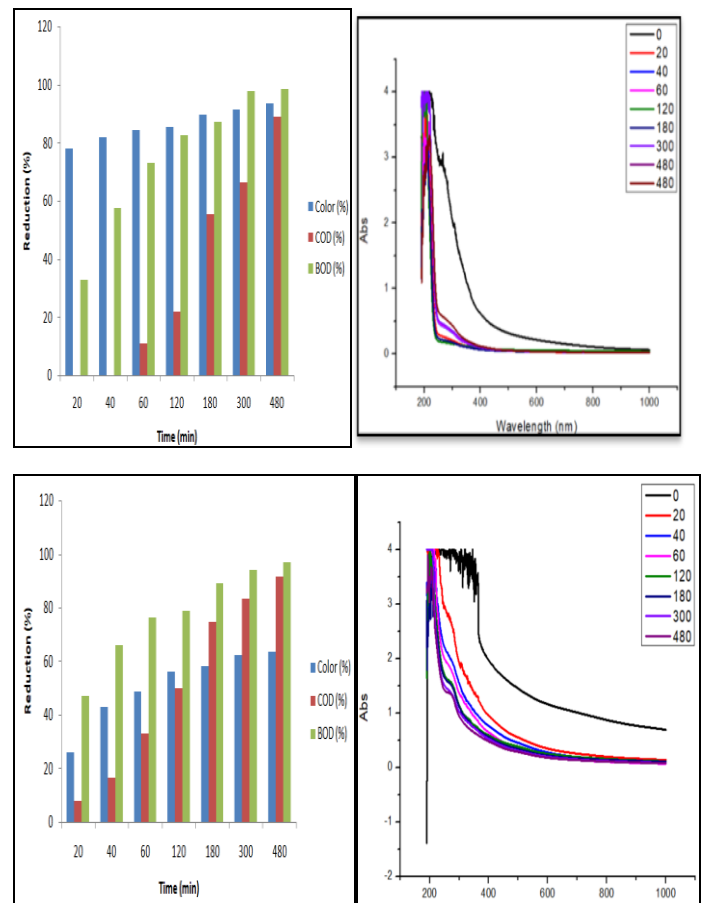


Fig 10 and 12: Reduction percentage of BOD, COD and color for 20 mg of BiFeO₃, Fig 11 and 13: Degradation for 20 mg of BiFeO₃ (250 nm)

3.4 Kinetic modeling

The photocatalytic activity of BiFeO₃ towards coffee effluent was fit using the Langmuir-Hinshelwood kinetic model under various treatment modalities using visible light irradiation (LED 9W) with 20 mg of dose (optimised) catalyst. The Langmuir-Hinshelwood model was used to match the photocatalytic activity of BiFeO₃ towards coffee effluent. In the kinetic plots (Figs. 6–13), the regression coefficients (R²) of each catalyst were reasonably close to 1, showing excellent linearity for all treatment options. Pseudo-first-order kinetic equations provide a good description of the dynamics of coffee effluent degradation catalyzed by BFO

in any treatment mode. The outcomes of pseudo-first-order kinetic modeling for the catalyst BiFeO₃ and the accompanying percentage of coffee effluent degradation are summarized in Table 4.2 and Figure 14, respectively. Arabica has the greatest R² value of 0.9767 and the highest rate constant of 0.004 min⁻¹. Robusta has an R² value of 0.9565 with a maximum rate constant of 0.005 min⁻¹. This is because the composite has a larger surface area, which enables it to absorb more light and enhances the effectiveness of the separation of photogenerated charges. According to photocatalysis investigations, the COD reaction rates for both Arabica and Robusta are significantly greater than those for BOD and colour catalysts in terms of kinetics.

Table 2: Pseudo-first-order rate constants (K_{app}), correlation coefficients (R^2), and degradation efficiency (%)

Coffee effluent	Parameter	K_{app} (min ⁻¹)	R^2	% Degradation
Arabica	BOD	0.00827	0.902	98.40
	COD	0.00479	0.976	88.88
	Color	0.00251	0.922	96.67
Robusta	BOD	0.00589	0.935	96.98
	COD	0.00533	0.956	91.66
	Color	0.00126	0.618	63.855

Experimental condition: Coffee effluent 100 mL; LED Bulb (9 W); 20 mg of BiFeO₃ catalyst

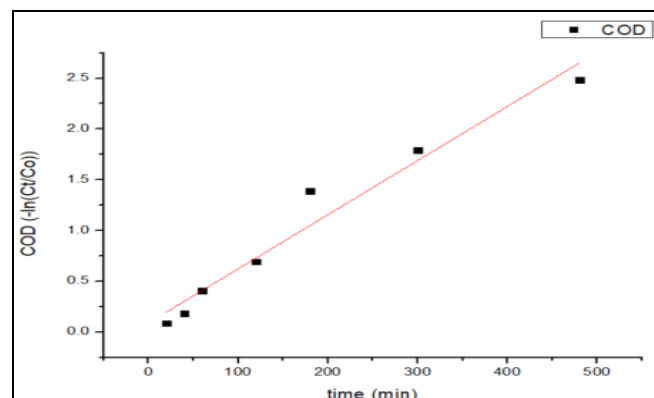


Fig 15: Kinetics for Robusta

4 CONCLUSIONS

Photocatalytic approaches are preferred above chemical, physical, and biological processes, all of which are viable possibilities, to degrade the primary organic pollutants. The findings of a physical and chemical analysis of coffee wastewater are summarized in Table 1. The study's results show that the BOD and COD levels in coffee effluent can rise to substantial levels, with values ranging from 3082 mg/l to 4082 mg/l and 7200 mg/l to 19200 mg/l, respectively. Additionally, the pH of the effluents varies from 3.59 to 4.58. It has been proven that the conversion of organic contaminants into non-hazardous byproducts via the photocatalytic degradation process is very effective. It is the most promising technology for getting rid of or deteriorating the organic pollutants that are currently present in the environment. Photocatalysis has the potential to produce power and hydrogen while lowering carbon dioxide emissions in addition to treating wastewater. In comparison to more conventional methods of pollution clearance, photocatalytic mineralization is more environmentally benign because of its ability to create water and carbon dioxide. BiFeO₃ is one of the best photocatalysts for wastewater degradation because of its nontoxicity, low bandgap energising energy, low cost, and long-term outstanding stability. Due to their effectiveness and speed, coprecipitation procedures were chosen for the production of BiFeO₃. Co-precipitation, which produces homogenous nanoparticles, can be used to swiftly and cheaply make nanoparticles. Due to its low evaporation temperature, bismuth poses one of the challenges in the production of bismuth ferrite. As a result of this procedure, secondary phases of bismuth ferrite are produced. This issue can be resolved using the co-precipitation method since it stops secondary phases from forming. Bismuth ferrite typically has particles that are less than 100 nm in size and is uniformly dispersed throughout. After an eight-hour contact time, a dose of 20 mg has been found to be the most efficient for treating coffee effluents. On the other hand, the Effluent Treatment Plant can only eliminate 78–80% of the BOD and COD present in coffee effluents. In contrast, 90–95% of each of these contaminants are removed through photocatalytic

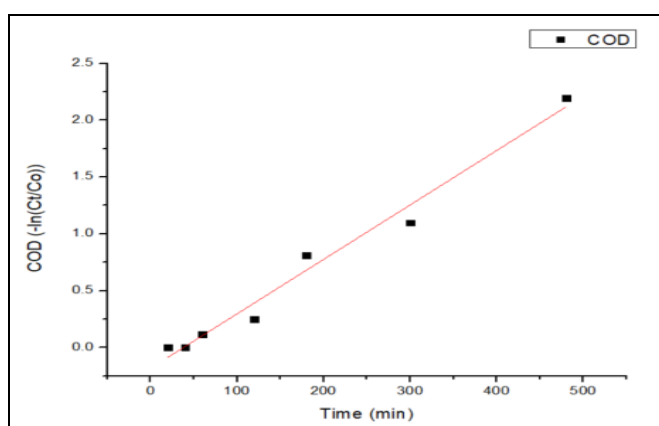


Fig 14: Kinetics for Arabica

degradation. Due to the presence of several macromolecules including caffeine, polyphenols, and various other compounds, coffee effluents have a high COD. Only 63 to 78% of the color can be removed from Robusta coffee, compared to 95 to 98% of the color from Arabica coffee. The reported photocatalytic reduction findings are best explained by the pseudo-first-order reaction kinetics model. For the kinetic investigation, we employed a model called the Langmuir-Hinshelwood model.

REFERENCES

- [1] A. Haruna, I. Abdulkadir, and S.O. Idris, (2020), "Photocatalytic activity and doping effects of BiFeO₃ nanoparticles in model organic dyes", Heliyon, 2020, Vol.6 <https://www.sciencedirect.com/science/article/pii/S2405844020300827>
- [2] Ammara Nazir, Shoomaila Latif, Syed Farooq Adil, Mufsir Kuniyil, Muhammad Imran, Mohammad Rafe Hatshan, Farah Kanwal and Baji Shaik, (2022), "Photocatalytic Degradation of Cefixime Trihydrate by Bismuth Ferrite Nanoparticles", Material, vol.15. <https://www.mdpi.com/1996-1944/15/1/213>
- [3] Asrat Gebremariam Woldesenbet, Belay Woldeyes, Bhagwan Singh Chandravanshi, (2014), "Characteristics of Wet Coffee Processing Waste and Its Environmental Impact in Ethiopia", International Journal of Research in Engineering and Science, vol.2(4):1-5. https://www.researchgate.net/publication/262311991_Characteristics_of_Wet_Coffee_Processing_Waste_and_Its_Environmental_Impact_in_Ethiopia
- [4] Bulent Caglar, Fatih İçer, Kemal Volkan Ozdokur, Sema Caglar, Agah Oktay Ozdemir, Eda Keles Guner, Burcu Meryem Bes,er, Ahmet Altay, Çağrı Çırak, Bilge Dogan, Ahmet Tabak, (2021), "A novel amperometric H₂O₂ biosensor constructed by cress peroxidase entrapped on BiFeO₃ nanoparticles", Materials Chemistry and Physics, vol.262. <https://www.sciencedirect.com/science/article/abs/pii/S0254058421000705>
- [5] Caglar, İçer, Ozdokur, Caglar, Ozdemir, Guner, Bes,er , Altay, Çırak, Dogan, Tabak. "A novel amperometric H₂O₂ biosensor constructed by cress peroxidase entrapped on BiFeO₃ nanoparticles", Materials Chemistry and Physics, 2021, vol.262. <https://www.sciencedirect.com/science/article/abs/pii/S0254058421000705>
- [6] Dr. T.N.Gopinandhan, Dr. J.S.Nagaraja, and Dr. Y. Raghuramulu, (2020), "Indian Coffee", The Coffee Magazine, vol.84 (12).
- [7] Dr. T.N.Gopinandhan, Dr. J.S.Nagaraja, T.N. Sandeep, Dr. H. Shruthi, Channabasamma B. Bided, and Dr. Y. Raghuramulu, (2020), "Indian Coffee", The Coffee Magazine, vol.84 (7). https://www.researchgate.net/publication/360099412_EVALUATION_OF_A_NEW_METHOD_FOR_TREATING_COFFEE_EFFLUENT
- [8] Fitria Ayu Sulistiani , Edi Suharyadi , Takeshi Kato and Satoshi Iwata, (2020), "Effects of NaOH Concentration and Temperature on Microstructures and Magnetic Properties of Bismuth Ferrite (BiFeO₃) Nanoparticles Synthesized by Coprecipitation Method", Key Engineering Materials, vol.855: 9-15. <https://www.scientific.net/KEM.855.9>
- [9] Gurudev Sujatha, Subramaniam Shanthakumar and Fulvia Chiampo, (2020), "UV Light-Irradiated Photocatalytic Degradation of Coffee Processing Wastewater Using TiO₂ as a Catalyst", Environments, vol.47 (7). <https://www.mdpi.com/2076-3298/7/6/47>
- [10] Hamed Maleki, Marzieh Haselpour¹ and Reza Fathi, (2017), "The effect of calcination conditions on structural and magnetic behavior of bismuth ferrite synthesized by co-precipitation method", Journal of Materials Science: Materials in Electronics, vol. 29: 4320-4326. <https://link.springer.com/article/10.1007/s10854-017-8379-z>
- [11] Malathia , Prabhakarn Arunachalamb, V.S. Kirankumar, J. Madhavana, Abdullah M. Al-Mayouf. "An efficient visible light driven bismuth ferrite incorporated bismuth oxyiodide (BiFeO₃/BiOI) composite photocatalytic material for degradation of pollutants", Optical Materials, 2018, vol.84: 227-235. <https://www.sciencedirect.com/science/article/abs/pii/S0925346718304488>
- [12] Nafees Ahmad, Jerry Anae, Mohammad Zain Khan, Suhail Sabir, Xiao Jin Yang, Vijay Kumar Thakur, Pablo Campo, Frederic Coulon, (2021), "Visible light-conducting polymer nanocomposites as efficient photocatalysts for the treatment of organic pollutants in wastewater", Journal of Environmental Management, vol.295. <https://www.sciencedirect.com/science/article/pii/S0304147921014249>
- [13] Ningappa Kumara Swamy, Kikkeri Narasimha Shetty Mohana and Shivamurthy Ravindra Yashas (2022), "GNR@CeO₂ heterojunction as a novel sonophotocatalyst: Degradation of tetracycline hydrochloride, kinetic modeling and synergistic effects", Colloids and Surfaces A: Physicochemical and Engineering Aspects, vol.639. [GNR@CeO₂ heterojunction as a novel sonophotocatalyst: Degradation of tetracycline hydrochloride, kinetic modeling and synergistic effects - ScienceDirect](https://www.sciencedirect.com/science/article/abs/pii/S0925346722000705)
- [14] Soltani, Mohammad H. Entezari. "Sono-synthesis of bismuth ferrite nanoparticles with high photocatalytic

activity in degradation of Rhodamine B under solar light irradiation”, Chemical Engineering Journal, 2013, Vol.223: 145-154. <https://www.sciencedirect.com/science/article/abs/pii/S1385894713003185>

[15] Xiong Wang, Ying Lin, Xifeng Ding and Jinguo Jiang, (2011), “Enhanced visible-light-response photocatalytic activity of bismuth ferrite nanoparticles”, Journal of Alloys and Compounds, vol.509: 6585-6588. <https://www.sciencedirect.com/science/article/abs/pii/S0925838811006591>

[16] Yaqoob, Parveen, Umar, and Ibrahim. “Role of Nanomaterials in the Treatment of Wastewater: A Review”, School of Chemical Sciences, 2020, Vol.12:495. <https://www.mdpi.com/2073-4441/12/2/4>